

See discussions, stats, and author profiles for this publication at: <https://www.researchgate.net/publication/245076744>

# Study of damage and repair of blades of a 300 kW wind turbine

Article in *Energy* · July 2008

DOI: 10.1016/j.energy.2008.02.002

CITATIONS

43

READS

2,907

4 authors, including:



J. C. Marín

University of Seville

15 PUBLICATIONS 357 CITATIONS

[SEE PROFILE](#)



A. Barroso

University of Seville

70 PUBLICATIONS 758 CITATIONS

[SEE PROFILE](#)

# Study of damage and repair of blades of a 300 kW wind turbine

J.C. Marín\*, A. Barroso, F. París, J. Cañas

*School of Engineering, University of Seville, Camino de los Descubrimientos s/n, 41092 Seville, Spain*

Received 6 September 2007

## Abstract

The inspection of damages detected in some blades of 300 kW wind turbines revealed that the nature of these damages was probably due to a fatigue mechanism. The causes that had originated the failure (superficial cracks, geometric concentrator, abrupt change of thickness) have been studied, verifying, by means of the simplified evaluation procedure of fatigue life of the “Germanischer Lloyd” (GL) standard, that these causes can explain the failure detected in the period of time in which it happened.

A suitable configuration for the repair of the damaged blades has been studied, by means of a finite element model. The proposed modifications repair the cracks and in addition contribute to relaxing the stress state in the affected zone. The introduction of a triangular reinforcement, which smoothes the re-entrant corner existing in the original design, incorporating a laminate of reinforcement, produces a significant decrease in the stress level in the damaged zone of the blades.

© 2008 Elsevier Ltd. All rights reserved.

**Keywords:** Wind turbine blade; Composites; Fatigue life; Repair; Finite elements

## 1. Introduction

The objective of the present work is the study and repair of the damages detected in the blades of 300 kW pitch control wind turbines fabricated by hand lay up. These damages, consisting of cracks located in the joining zone of the blade with the root, appeared over short periods of time (around five years with an average measured number of  $14.26 \times 10^6$  cycles per year) and systematically in blades in which fatigue loads were more severe. Similar damages appeared also, but over longer periods of time, in blades under more benign fatigue conditions. In any case, these periods were inferior to the design life of the blades (20 years). In this work, the reasons lying behind the damages detected are studied, to be used as a basis for repairing similarly affected blades.

First, a complete inspection of the damaged zone of the blade was carried out, cutting this damaged zone to evaluate the nature of the damage and to observe the inner structure of the zone. The correct correspondence of the structure of the laminates with that established at design as

well as the existence of possible defects of manufacture is verified. The results of this visual inspection allow a qualitative estimation of the causes, which could originate the appearance of the cracks to be performed.

The quantitative justification of the viability of the appearance of the failure observed, in the period of time detected, has been carried out using the simplified model of the Germanischer Lloyd (GL) standard.

In order to support the proposal for repair of the damaged blades, several modifications to the original conception of the blade have been studied by means of numerical analysis (finite elements), the influence that these modifications have on the local stress state responsible for the failure being evaluated. Finally, the way to materialize these modifications in the practical repair of the blades is studied.

## 2. Visual inspection of the cracks and analysis of laminates

A picture of the typical damage found in a blade, in the form of cracks on the external surface, is presented in Fig. 1. The crack is located in the transition zone between the root of the blade and the zone of aerofoil profile. The cross-sectional section of the blade in the aerodynamic

\*Corresponding author. Tel.: +34 954487299; fax: +34 954461637.

E-mail address: [jcmarin@esi.us.es](mailto:jcmarin@esi.us.es) (J.C. Marín).

zone is a thin-walled section that reproduces the aerofoil profile and presents a vertical partition (denominated spline) that divides the section into two cells: leading edge and trailing edge (Fig. 2). The cross section in the root zone is practically cylindrical.

The transition between the root zone and the aerodynamic zone is made in such a way that the cylindrical root geometry is progressively transformed into the cell of the leading edge that constitutes the resistant part of the section. The cell of the trailing edge is closed in the zone of transition by means of an element triangular in shape, constituted by a laminate of low resistance, an element which we will refer to in what follows as cover. As can be observed in Fig. 1, the crack extends throughout both the union cover-root and the transition root-aerodynamic zone.

In order to have a visual inspection of the failure area, it is divided into slices of 2–3 cm width, as shown in Fig. 3a and b, so that the progression of the internal damage can be observed. A detail of the damaged area at slice number 7 is shown in Fig. 3c, whereas those areas corresponding to slices number 6 (left) and number 5 (right) are shown in Fig. 3d.

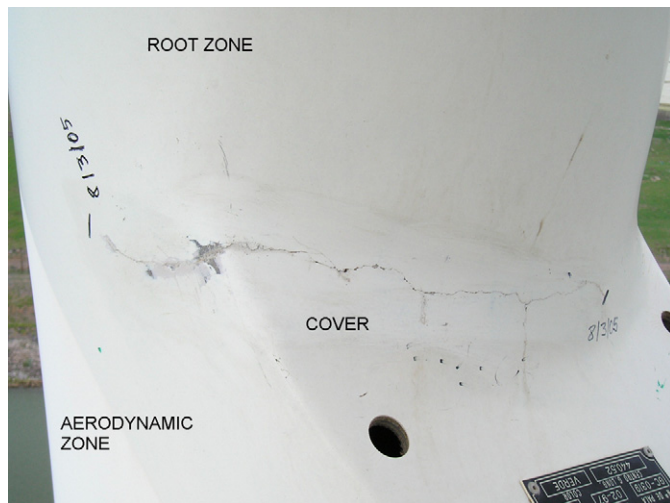


Fig. 1. Location of the cracks on the surface of a blade.

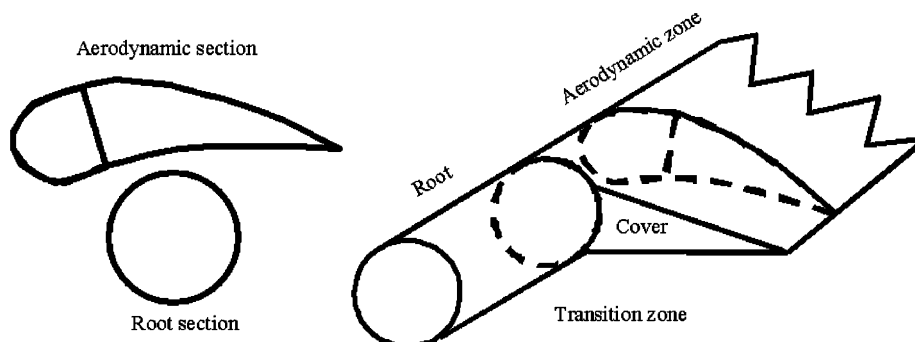


Fig. 2. Scheme of the blade geometry.

Although the evolution of damage is difficult to establish, the crack observed in the inspection (see Fig. 1) is formed by several well-differentiated parts: (a) the part that runs through the cover (slices 8 and 9), which affects the whole thickness of a laminate without resistant function, (b) the continuation of this part on slice 7 which only affects the external layers of the laminate, with breaking of unidirectional fibres and multiple delaminations (as can be observed in Fig. 3c), (c) the part corresponding to slices 5 and 6 in which the whole thickness is damaged (as observed in Fig. 3d) and finally (d) slice 4, where the actual crack front is located, as no appreciable damage is observed at the side facing slice 3. Notice that the fabrication defects observed appear at slices 8 and 9, slices 5 and 6 where the damage starts to develop being free of initial manufacturing defect.

The following information can be deduced from the inspection of the samples:

- An *a posteriori* lamination over the gel coat on the external surface and centred in the area of the crack (see Fig. 3d) can be observed.
- An abrupt change in the thickness of the laminate exists in the area of the crack (see Fig. 3b and d for more details) the difference of thickness being in some cases (slice 5) up to 10 mm, from 17 to 27 mm, over a distance of only 150 mm.
- The presence of areas with lack of resin (see Fig. 3b and c).
- A debonding is observed between the spline and the aerodynamic walls (when the whole set is looked at from the upper part).

Calcinations of laminate samples from slice 5 were carried out in a muffle oven at 600 °C for 90 min to obtain the real stacking sequence on both sides of the crack. After the calcination of the resin, the layers defining the laminate are shown in Fig. 4. The stacking sequence observed after the calcinations is shown in Table 1, where MAT indicates layers of short fibre randomly distributed, NUFF represents unidirectional layers oriented at 0° with respect to the longitudinal direction, TRIAX represents triaxial layers 90/45/−45, BIAX represents biaxial layers 0/90 and/or 45/−45, and GEL denotes the external layer of gel coat.

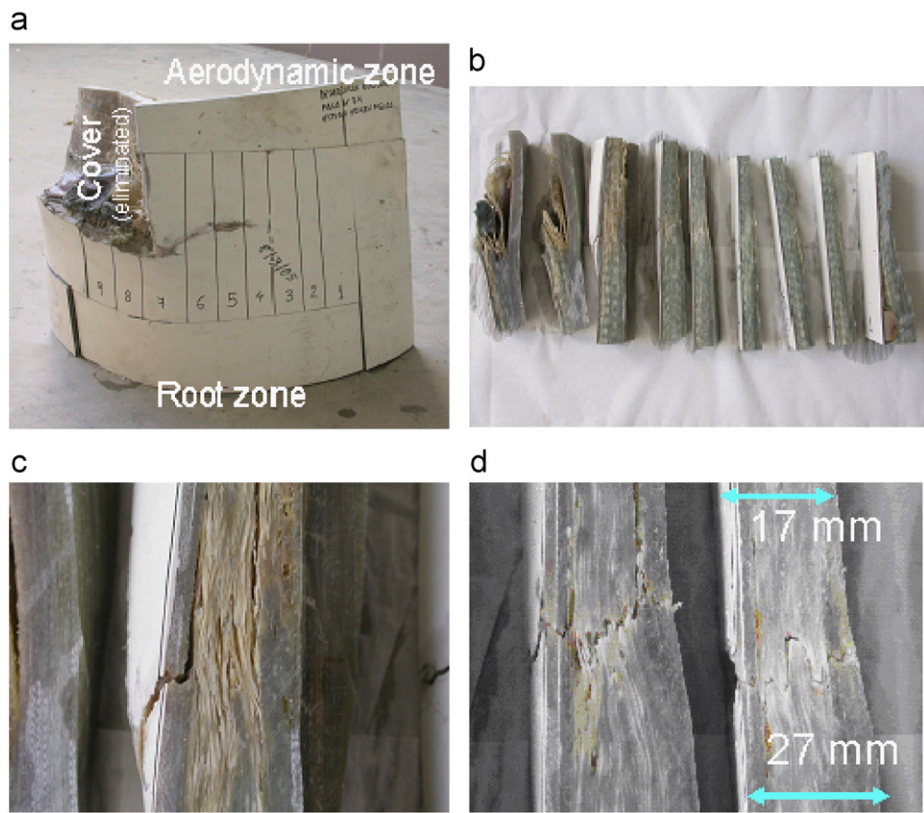


Fig. 3. Details of the internal damage suffered by the blade.



Fig. 4. Stacking sequence of the laminate.

Table 1  
Laminate obtained in the calcinated samples

Laminate of root part	GEL	1 MAT	1 TRIAX	13 NUFF	1 BIAX	4 NUFF	1 MAT	1 TRIAX	3 BIAX	1 TRIAX
-----------------------	-----	----------	------------	------------	-----------	-----------	----------	------------	-----------	------------

The most noticeable result is the difference in the number of unidirectional layers (in a proportion of 17 to 10) from the root zone to the aerodynamic area. Also noticeable is the presence of several biaxial 0/90 layers and one triaxial layer inside the root part that do not appear in the aerodynamic part.

Comparing the laminate found in the calcinated samples with the laminate that is described in the lamination manual, an excellent agreement is observed in the laminate of the aerodynamic part, whereas the laminate of the root part presents in the sample several additional layers of NUFF in comparison with that prescribed in the lamination manual. This increment of layers observed may be

motivated by the existence of overlap in circumferential direction in the disposition of the layers in the laminate of the root (Fig. 5b).

3. Evaluation of the causes of damage

After the visual inspection carried out, the causes most likely to have played a significant role in the origin of the detected damage are: the abrupt change of thickness observed, the local geometry of stress concentrator in the transition area and the observed defects of manufacture of the blade. These factors are discussed separately in what follows.

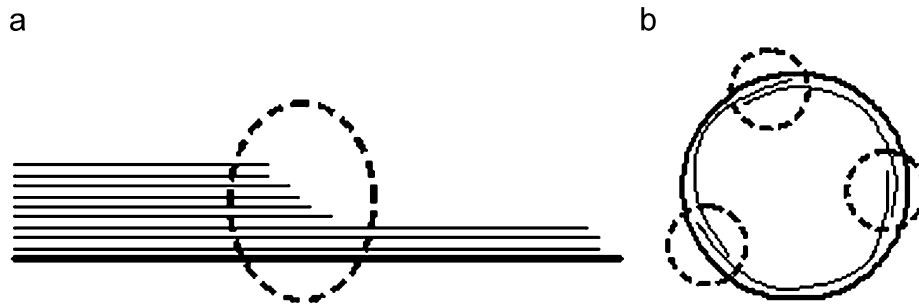


Fig. 5. Changes of thickness motivated by the reinforcements. a: longitudinal reinforcements; b: overlaps of the circumferential reinforcements.

### 3.1. Abrupt change of thickness

The most damaged zone from a structural point of view is the one between slices 5 and 6, in which the damage affects the whole thickness of the laminate, whereas the crack does not cross the whole thickness in slice 7.

It is in these slices (5 and 6) that, after the inspection carried out in Section 2, a more marked transition in thickness can be observed (Fig. 3). This abrupt change of thickness produces an eccentricity in the transmission of the load, generating bending moments that make the laminate not work uniformly over the whole thickness. Additionally, the unidirectional layers that are present in both laminates suffer misalignment in the longitudinal orientation of the fibre. This misalignment, under compression, can accentuate the failure mechanisms associated to local micro-buckling of the fibre.

Internal discontinuities also appear in the laminate in this area of thickness change. They are provoked by the end of a layer (Fig. 5a), a circumstance habitually referenced in the literature as “ply drop” [1]. An accumulation of these internal defects could favour the appearance and propagation of greater defects.

### 3.2. Local geometry of stress concentrator

The abrupt transition between the root area and the aerodynamic area generates a local geometry of re-entrant corner, undesirable from a structural point of view since it acts as local stress concentrator. The root area being the most loaded in the whole blade, the presence of concentrators that amplify the efforts on the laminate results in the existence of critical points for the beginning of failure.

### 3.3. Lack of resin and debonding manufacture defects

The joints are the weakest points in all structures. If additionally these joints are associated with the presence of defects, this weakness is consequently accentuated. The corner between the cover, the root and the aerodynamic area presents manufacture defects associated to the lack of resin (see slice 7) and debonding defects associated to the curing process (see slices 8 and 9).

Although the resin does not have the mechanical properties of the fibres, a laminate with lack of resin does not work as a unique material, its carrying load capacity, mainly under compression, diminishing noticeably.

### 3.4. Evaluation of the problem

Although the reasons set out above do not by themselves fully explain the appearance of the premature failure observed, the combination of the three, in the area of the blade with most stress requirements, can represent sufficient reasons for the premature failure of the blade.

The damage is clearly motivated by a mechanism of fatigue. A prediction of fatigue life is always based on the consideration of a material without defects, the lack of resin and the observed defects accelerating this failure mechanism. Additionally, the combined effect of the geometry of the concentrator and the abrupt change of thickness amplifies the efforts that act locally in an area, which in addition to suffering the greatest efforts along the whole blade, presents apparent damage.

The quantitative influence on the fatigue life of the blade of each one of these previously described aspects will be evaluated in the following section. The particular objective is to find, with the knowledge we have about the location of the damage, the approximate period of time before its appearance, and regarding the failure mechanism, under what hypothesis it is reasonable to justify quantitatively a fatigue failure such as the one observed.

## 4. Justification of the failure

Current knowledge of fatigue failure in laminates of composite materials is, in comparison with metallic materials, certainly limited, due to the more recent development of composites and to their greater complexity, in particular, regarding failure mechanisms. A fatigue analysis requires, besides a detailed description of the loads spectrum, a deep knowledge of the fatigue behaviour of the material [2]. In this sense the information which is being generated (see for instance DOE/MSU Fatigue Database [3], “Fatigue of materials and components for wind turbine rotor blades” [4]), to simulate the behaviour under fatigue of the materials used in the building of wind turbine blades,



is necessary to advance in the analysis and design of these elements.

Although the appearance of the damage leads to consider fatigue as the cause of the failure, a classical static analysis was carried out using nominal loads in accordance with GL [5]. The results, not included in the paper for the sake of brevity, showed that the stresses under these loads were far from their allowable values and consequently the static loads had no responsibility on the observed failure.

In this section, the estimation of the fatigue life, in order to elucidate if the detected failure can be justified based on the actual configuration of the blade, will be carried out. The simplified procedure proposed in the GL standard [5] (which is one of the most extensive and most specific procedures for the design and certification of these elements) will be used. Although more refined treatments for composite fatigue design [6–9] are available, the GL procedure satisfies the requirements of this study.

#### 4.1. Calculation of fatigue life by means of simplified spectrum according to GL

The GL strength verification adopts the following general expression:

$$S \leq \frac{R_k}{\gamma_{mx}} = R_d \quad (4.1)$$

where  $S$ , which represents the stress associated to a load case, cannot overcome the design strength  $R_d$ , which is obtained from decreasing the strength of the material  $R_k$  by means of a safety factor that adopts, depending on the case, the values:

$$\text{for the static analysis : } \gamma_{ma} = 2.67 \quad (4.2)$$

$$\text{for the fatigue analysis : } \gamma_{mb} = 1.485 \quad (4.3)$$

The load spectrum to be used could be obtained from real measurements or using simulation techniques. The simplified spectrum shown in Fig. 6, which constitutes

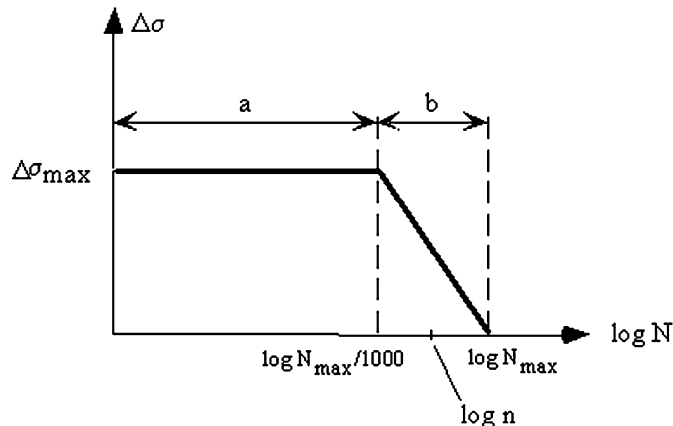


Fig. 6. Simplified spectrum of loads for the calculation of fatigue life.

a conservative option versus the previous ones, will be used. This spectrum is built up using the stresses corresponding to the case N1.0 of GL, called “basic state power production” which includes aerodynamic, inertia (gravity, centrifugal and gyroscopic) and functional forces. The range of stresses  $\Delta\sigma = |\sigma_{max} - \sigma_{min}|$  is represented versus the number of cycles in logarithmic scale,  $\log N$ ,  $N_{max}$  representing an estimation of the blade fatigue life.

Two well-differentiated areas can be clearly detected in Fig. 6:

*Area a:* where a maximum range  $\Delta\sigma_{max} = 1.5 \cdot \bar{\sigma}$  is assumed,  $\bar{\sigma}$  being the average value of stresses originated by the forces associated to load case N1.0. The duration in cycles of this part of the spectrum, for a total life of  $N_{max} = 10^x$ , is  $10^{x-3}$ .

*Area b:* which includes the rest of the cycles up to  $10^x$ , with stress ranges according to the equation:

$$\Delta\sigma = 0.5 \cdot \bar{\sigma} \cdot \log\left(\frac{N_{max}}{n}\right) \quad (4.4)$$

for  $\log\left(\frac{N_{max}}{1000}\right) \leq \log n \leq \log N_{max}$

The fatigue life calculation, which of course is made using the most unfavourable value of  $\bar{\sigma}$ , is based on the S–N curve of the laminate and on the Goodman diagram built from it, Fig. 7. As S–N curves are not available for all the different laminates, and to obtain them experimentally is non-viable from a practical point of view, the GL standard proposes the use of:

$$\Delta\sigma = \frac{2 \cdot \sigma_s}{\gamma_{mb} \cdot N^{1/9}} \quad (4.5)$$

$$\Delta\sigma^o = \frac{\Delta\sigma}{1 - ((\bar{\sigma} \cdot \gamma_{ma})/\sigma_s)} \quad (4.6)$$

where  $\sigma_s$  is the laminate strength (corresponding to the stress component under consideration),  $N$  is the number of cycles,  $\Delta\sigma = |\sigma_{max} - \sigma_{min}|$  the stress range and  $\gamma_{ma}$  and  $\gamma_{mb}$  are, respectively, the static and fatigue safety factors.

The fatigue life can be calculated using these diagrams, evaluating the accumulated damage  $D$ , by Miner’s rule, as

$$D = \sum_i \frac{n_i}{N_i} \quad (4.7)$$

where  $n_i$  is the load cycles number for a stress range  $i$  and  $N_i$  is the allowable load cycles number associated to  $i$ .

Substituting the expression of the Goodman diagram in the S–N curve, the expression that provides  $N_i$  for a determined stress range is obtained:

$$N = \left[ \frac{2}{\gamma_{mb}} \left( \frac{\sigma_s}{\Delta\sigma} - \frac{\bar{\sigma} \cdot \gamma_{ma}}{\Delta\sigma} \right) \right]^9 \quad (4.8)$$

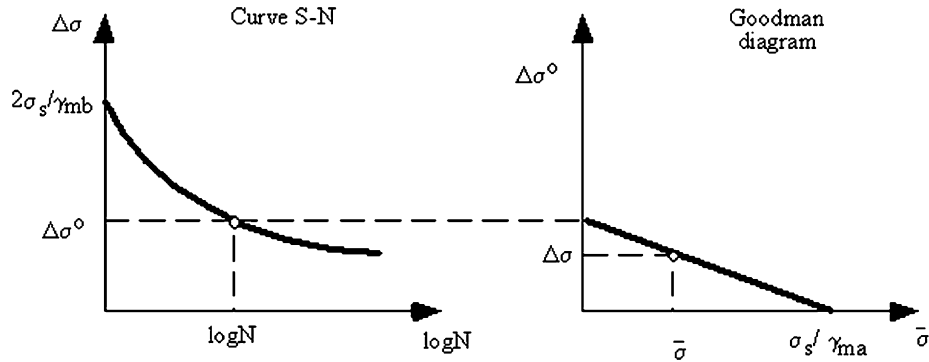


Fig. 7. S–N curve and Goodman diagram.

The first area of the spectrum (a) with a constant stress range contributes to the accumulated damage with  $n_1/N_1$ :

$$N_1 = \left[ \frac{2}{\gamma_{mb}} \left( \frac{\sigma_s}{1.5 \cdot \bar{\sigma}} - \frac{\gamma_{ma}}{1.5} \right) \right]^9, \quad n_1 = \frac{N_{max}}{1000}$$

$$\frac{n_1}{N_1} = 2.6368 \times 10^{-3} \frac{N_{max}}{((\sigma_s/\bar{\sigma}) - \gamma_{ma})^9} \quad (4.9)$$

The rest of the spectrum contributes with  $\int_{N_{max}/1000}^{N_{max}} (dn/N)$ , where introducing the expression of  $N$  the following expression can be obtained:

$$\int_{N_{max}/1000}^{N_{max}} \frac{dn}{N} = 4.2824 \times 10^{-3} \frac{N_{max}}{((\sigma_s/\bar{\sigma}) - \gamma_{ma})^9} \quad (4.10)$$

The complete expression of the accumulated damage is

$$D = 6.919 \times 10^{-3} \frac{N_{max}}{((\sigma_s/\bar{\sigma}) - 2.67)^9} \quad (4.11)$$

an expression which allows the fatigue life corresponding to an accumulated damage equal to  $D = 1$  to be calculated. The measured relationship between the number of cycles and the years of operation for the blades under study is  $14.26 \times 10^6$  cycles/year. Using this relationship, the equivalence between cycles and years of life for certain periods of time is shown in Table 2.

As is deduced from expression (4.11), in accordance with the simplified treatment adopted, the prediction of fatigue life at a certain point of the blade depends exclusively on the relationship between the strength of the laminate and the value of the average stress existing at this point. Hence, in the following sections, the value of these magnitudes will be analysed in the area affected by the failure.

#### 4.2. Evaluation of the laminate strength

It should be pointed out that when speaking of  $R_k$  as the characteristic strength of the material, this refers to the complete laminate. The values of  $R_k$  ought to be obtained by testing the different laminates of the blade. This is not practical, due first of all to the number of different stacking sequences of the blade and secondly to the fact that the failure load of most laminates exceeds the load capacity of most conventional testing machines. As an alternative, an

Table 2

Equivalence between number of cycles and years

No. of cycles	$0.43 \times 10^8$	$0.57 \times 10^8$	$0.71 \times 10^8$
Years	3	4	5

empiric rule has been used to evaluate the strength of the laminate working from the strengths of the component layers. This approach has been contrasted with experimental results and with models of progressive failure [10] by means of degradation properties [11,12], a good agreement being obtained. The expression used is

$$\sigma_{allowable\_i} = \frac{\sum_n \sigma_{allowable\_n} \cdot t_{ni}}{t_i} \quad (4.12)$$

where  $\sigma_{allowable\_i}$  is the strength of the  $i$ th laminate,  $\sigma_{allowable\_n}$  is the strength of a layer or a group of layers (the summation extends in  $n$  to all layers, or groups, with different strengths: NUFF, DDB, Biaxial 0/90, MAT and balsa wood),  $t_{ni}$  is the thickness of material  $n$  present in the laminate and finally  $t_i$  is the total thickness of the laminate.

Using expression (4.12), with the stacking sequence deduced after the calcination tests (Section 2), and using the allowable values (evaluated experimentally) of each one of the component layers, as well as its thickness, the allowable stress of the laminate corresponding to the section of smaller thickness of slice 5 (damaged zone) can be evaluated. The allowable (tensile strength) of each layer appears in Table 3. Based on these allowables, a value of 417.1 MPa is obtained for the allowable of the laminate.

It is necessary to consider the appropriate strength value of the laminate to be used in the analysis. To this end, it has to be pointed out that, although the predominant form of work in the area in question is under tension (98%, experimentally measured), a certain percentage also takes place under compression (2%). This fact, knowing the different fatigue behaviour under tension and compression, will be taken into consideration in what follows.

A series of compression tests on unidirectional (NUFF) specimens, which is the component that predominantly characterizes the resistant behaviour of the laminates of the blade, were carried out. The specimens were made of a

Table 3

Allowable values (tensile strength), thicknesses and properties of the different types of layers

Material	$\sigma_{allowable}$ (MPa)	Thickness (mm)	$E_{11}$ (GPa)	$E_{22}$ (GPa)	$G_{12}$ (GPa)	$\nu_{12}$
NUFF (unidirectional)	501.3	$1.333 \times 10 = 13.33$	34.5	9.34	2.7	0.35
DDB (tri-axial 90/45/−45)	74.1	$1.034 + 0.554 \times 2 = 2.142$	27.1	7.3	2.1	0.35
DB (bi-axial +45/−45)	112.5	$0.314 \times 2 = 0.628$	27.1	7.3	2.1	0.35
MAT (random)	124.9	$0.460 + 0.214 = 0.674$	9.78	9.78	3.7	0.32

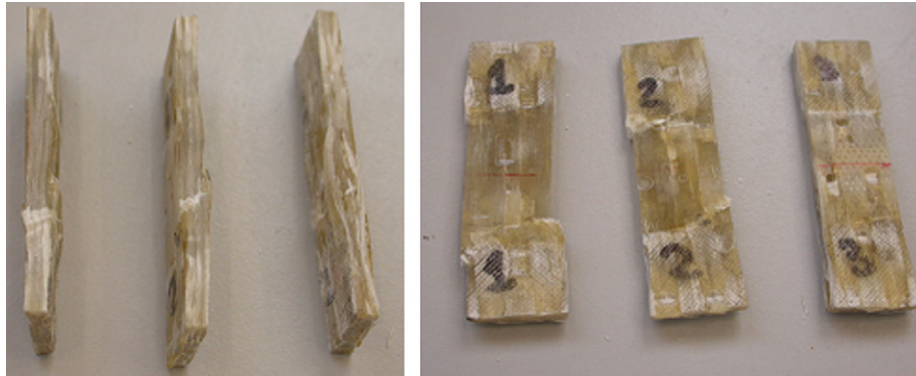


Fig. 8. Compression tests of unidirectional laminates.

laminate of glass fibre vinylester resin with three layers of NUFF 1450, the total thickness being 3.99 mm. The tests were carried out in an INSTRON 8801 (100 kN). The tested specimens are shown in Fig. 8, the experienced failure type being associated to a phenomenon of micro-buckling of the fibres, which is favoured by the longitudinal waving of the tows of the fibres present in these materials.

The measured average value of the compression strength is 250.9 MPa, presenting a typical deviation of 23.7 and a coefficient of variation of 9.45%. Starting from these values, and applying the statistical treatment that recommends the GL standard, the characteristic value of the compression strength of the NUFF layers would be 189.4 MPa. Therefore, the relationship between the characteristic values of the tensile and compressive strength of the unidirectional (NUFF) layers is 2.65.

Given the predominant character of the unidirectional layers in the resistance in longitudinal direction of the laminate, it would be acceptable to suppose that the relationship between the strength to tension and compression of the laminate follows the same proportion as that corresponding to the layers of NUFF. Based on this hypothesis we can estimate the value of the characteristic compression strength of the laminate under question, which would be 157.4 MPa.

Bearing in mind the fact that part of the life of the element works in tension and another part in compression, the correct treatment would involve using the strengths to tension and compression, respectively, for the corresponding parts of the life of the element. In this case, due to the fact that a simplified spectrum, where it is not possible to distinguish between work in tension and compression, will be used, it has been considered appropriate to modify the

value of the allowable stress to be used for the fatigue calculation. To this end, the allowable stress of the laminate will be evaluated as the average value between the tension (417.1 MPa) value and that of compression (157.4 MPa) weighted by the respective work percentages, that is  $\sigma_{allowable} = 411.9$  MPa. It should be pointed out that this small variation in the allowable stress, which could be considered worthless to static effects, has a considerable influence on the fatigue life prediction.

Only reference to normal stresses has been made in the former discussion due to the fact that shear stresses are almost negligible in the zone under consideration, the laminate having in any case [+45/−45] layers (BIAX) to support these stresses.

#### 4.3. Evaluation of the average stress of the laminate

The value of the nominal average stress at the neighbourhood of the affected zone has been evaluated by means of a model based on the Strength of Materials Theory [13] that considers the characteristics of the laminates (by means of the Classic Theory of Laminates) and the geometric configuration of the section. The load hypothesis considered is case N1.0 of GL standard. The value of the obtained nominal average stress is  $\bar{\sigma} = 10.77$  MPa. This nominal value can be affected by the change in thickness of the laminate and by the existing concentrator in the transition zone.

The difference in thickness between the adjacent laminates produces an eccentricity of the transferred load, which causes the appearance of a bending moment that amplifies the longitudinal normal stress. This effect will be evaluated using the scheme shown in Fig. 9.



The moment  $N_x \cdot d$  created by the eccentricity of the load must be absorbed by the laminates. The most unfavourable case is that in which the laminate of smaller thickness absorbs it completely, the maximum normal stress being

$$\begin{aligned}\sigma_{max} &= \frac{N_x}{e} + \frac{N_x \cdot d}{\frac{1}{2}e^3} \frac{e}{2} = \frac{N_x}{e} \left[ 1 + 6 \frac{d}{e} \right] \\ &= \frac{N_x}{e} \left[ 1 + 6 \frac{4.7}{17.9} \right] = \frac{N_x}{e} [1 + 1.57] = 2.57 \frac{N_x}{e} \quad (4.13)\end{aligned}$$

If, on the other hand, the moment is distributed in the laminates proportionally to their bending stiffness, the minimum value of normal stress for each one of the ends is obtained, its expression being

$$\sigma_{max} = \frac{N_x}{e} + \frac{1}{6} \frac{N_x \cdot d}{\frac{1}{2}e^3} \frac{e}{2} = \frac{N_x}{e} [1 + 0.26] = 1.26 \frac{N_x}{e} \quad (4.14)$$

Therefore, the effect of the change in thickness on the laminates involves an amplification of the normal stress,

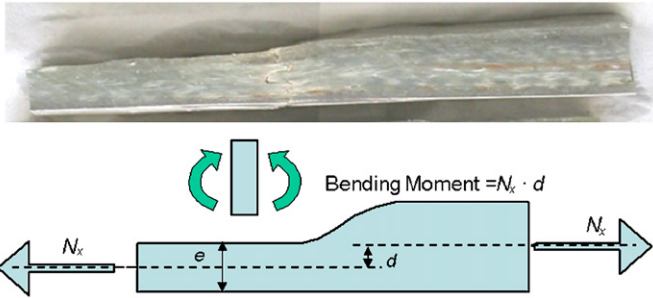


Fig. 9. Evaluation of the influence of the change in thickness.

whose effect can be quantified by a factor, its value being reasonably comprised between 1.26 and 2.57. With the nominal stress  $\bar{\sigma} = 10.77$  MPa and applying the obtained factors, the value of the normal stress would be in the range between 13.6 and 27.7 MPa.

Due to the geometric configuration of the design of the blade, the point under study is within the zone of influence of the concentrator described in Section 3.2, so that the total normal stress would be affected by a concentration factor associated to this geometry. This factor depends on the real configuration of the geometric detail existing at each blade and therefore on the manufacture process. The total normal longitudinal stress is then calculated multiplying the nominal average stress by the factor of amplification due to bending  $f_{bend}$  and by the factor of amplification due to the concentrator  $f_{conc}$ :

$$\bar{\sigma}_{real} = \bar{\sigma} \cdot f_{bend} \cdot f_{conc} \quad (4.15)$$

Finally, it is necessary to take into consideration that when the laminate is going to suffer the failure of the resistant layer, the external layer presents a crack, motivated by the effect of the concentrator, described in Section 3.2, on the weak laminate of the cover, as is indicated in Fig. 10a.

The effect of this superficial crack on the stress state is double. First, the value of the nominal average stress is increased by the loss of thickness implied by the existence of cracked layers, varying from  $\bar{\sigma} = 10.77$  to 11.82 MPa. Second, it would imply, strictly speaking, an intensification of the stresses at the tip of the crack. This effect will, for simplicity, be taken as a concentration of the stresses, being included within the factor  $f_{conc}$  of expression (4.15).

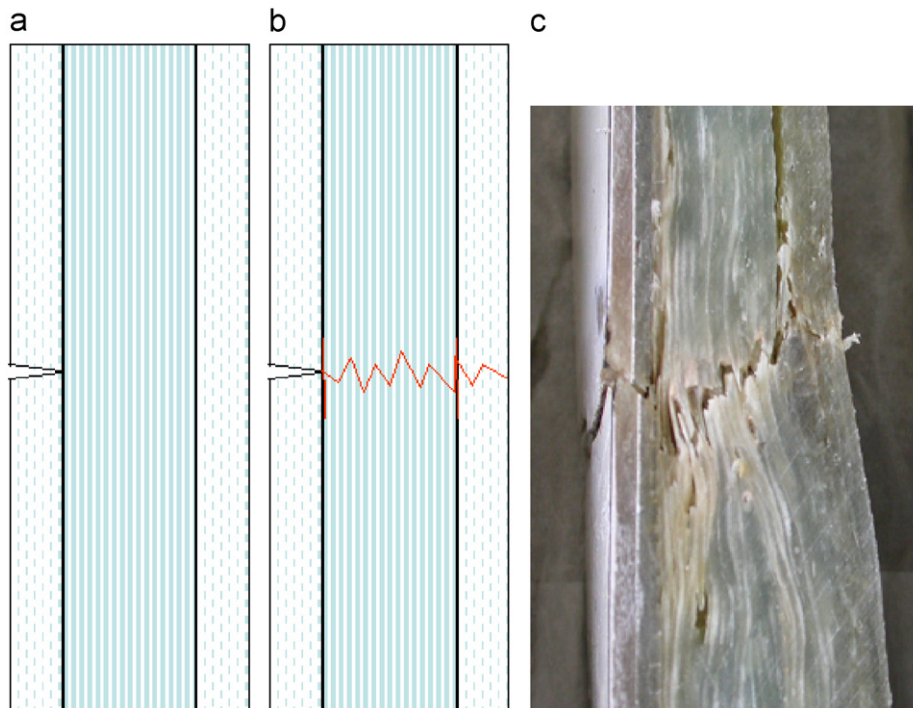


Fig. 10. Scheme of the progression of the crack in the laminate: (a) crack in the superficial layer, (b) crack in the resistant layer and (c) view of the real crack.

#### 4.4. Evaluation of fatigue life

Once the previous considerations have been made, with regard to the laminate strength and the normal longitudinal average stress appearing at the zone of study, an estimation of the fatigue life can be carried out.

Taking expression (4.11), which evaluates the fatigue life, and introducing  $\sigma_s = 411.9 \text{ MPa}$  (see Section 4.3) and  $N_{max} = 0.71 \times 10^8$ , corresponding to a life of 5 years (see Table 2), which is approximately the observed life of the blade under study, the values of the average stress that would cause the fatigue failure, that is  $D = 1$ , can be estimated. The normal longitudinal average stress obtained by means of the described procedure is  $\bar{\sigma}_{real} = 59.2 \text{ MPa}$ .

Using expression (4.15), with an average stress of  $\bar{\sigma} = 11.82 \text{ MPa}$ , and knowing that the reasonable range of variation of the factor  $f_{bend}$  is from 1.26 to 2.57, the factor  $f_{conc}$  (due to the geometric concentrator and to the presence of the superficial crack) that causes a real average stress of  $59.2 \text{ MPa}$  would then be between 1.95 and 3.97.

The obtained values are of a similar order of magnitude to those associated to a geometric concentrator like the one appearing at the root of the blade. In order to evaluate quantitatively the range of values of this concentrator, solutions of similar problems (see Fig. 11a) can be found in the literature [14, pp. 286–287]. In particular, two problems with similar geometry to the real concentrator have been taken, corresponding to tension (Fig. 11c) and bending (Fig. 11d) loads.

The parameters on which the stress concentration factor depends can be estimated, for the dimensions of the blade (Fig. 11b), within the following ranges:

$$15 < h/r < 20; \quad 0.3 < 2h/D < 0.4 \quad (4.16)$$

where  $r$  is the radius of curvature,  $D$  and  $d$  are the characteristic dimensions at both sides of the concentrator and  $h$  is the difference between  $D$  and  $d$ .

Using the previous values for the calculation of the stress concentration factor ( $f_{conc}$ ), the following ranges for the

cases of tension and bending are obtained:

$$\text{tension : } 3.01 < f_{conc} < 3.59$$

$$\text{bending : } 2.94 < f_{conc} < 3.60 \quad (4.17)$$

The range of values calculated for  $f_{conc}$  is, as can be observed, within the interval of values previously obtained (1.95–3.97), values that can reasonably cause the fatigue failure in the period of time considered.

Additionally, using the finite element model (which will be detailed later on) of the original configuration that will be used in the analysis of the modifications to be performed on the blades, an estimation of the longitudinal average stress in the zone under study can be obtained, since this point is relatively far from the corner (around 10 cm). The value of the longitudinal average stress at the point considered is  $26.43 \text{ MPa}$ . If this value is compared with the nominal average stress previously evaluated  $\bar{\sigma} = 10.77 \text{ MPa}$  (considering that in the numerical model the existence of cracked layers is not contemplated), a stress amplification of 2.45 is obtained, which is within the interval of values previously found (1.95–3.97). This fact corroborates that the actual stress level could reasonably cause the fatigue failure in the period of time considered.

#### 5. Concentrator geometry influence

Once the causes of the damage have been detected, the design of a suitable repair to stitch the existing cracks in the damaged blades and to relax the stress state in order to prevent similar failures, constitutes the next step in the study.

In order to diminish the stress state in the area where the failure appeared, the influence that a variation in the local geometry of the concentrator has on the stress state, and therefore on an improvement of the fatigue life, will be studied. This analysis will be carried out by means of finite elements, using ANSYS [15], and attempts to modify the geometry of re-entrant corner that appears at the beginning

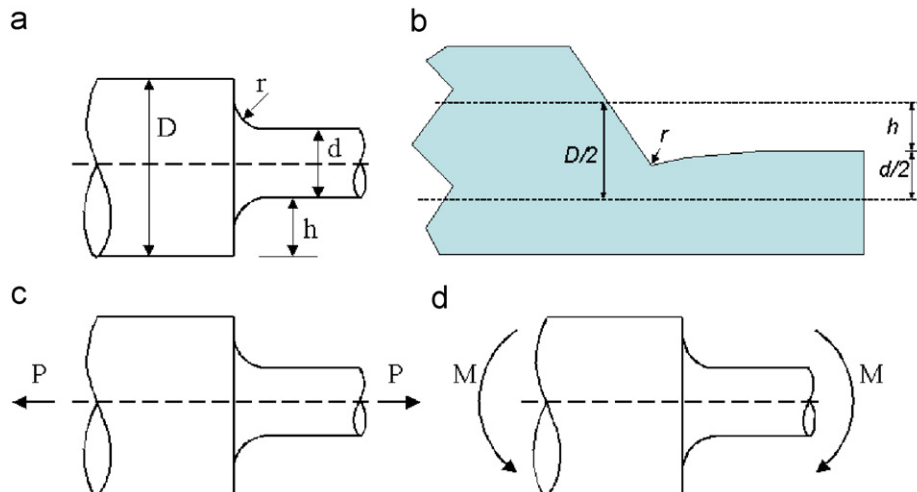


Fig. 11. Geometric scheme of the concentrator. a: simplified scheme; b: blade dimensions; c: tension problem; d: bending problem.

of the aerodynamic zone, smoothing the angle of this corner. This modification follows the present tendency in the design of wind turbine blades, in which this transition is made much more smoothly than is the case of the blade under consideration.

Two configurations have been proposed to smooth the geometry of the above-described concentrator. In Fig. 12, by means of finite element models, a detail of the zone under study is shown in its original conception (a), and in two modified versions, (b) and (c), susceptible of being easily implemented in the blade.

The numerical model of the original geometry is described in detail in Section 5.1, whereas those associated to the two proposed modifications are described, respectively, in Section 5.2. A summary of the obtained results will be presented in Section 5.3.

### 5.1. FEM model. Original geometry

The model performed by ANSYS uses shell elements (shell99), which allow orthotropic materials to be used and the stacking sequence of the laminates (up to 100 layers) to be defined. Shell99 is a quadrilateral element of eight nodes, four in the vertices and four at the midpoints of each edge. Each node has six degrees of freedom (three displacements and three rotations). The model consists of 5380 nodes and 2027 elements, more than 500 types of different stacking sequences having been defined. The blade has been divided into 64 sections along the longitudinal direction. The nodes at the first section have the displacements restricted, so that the blade is clamped at the root end. This model has been previously validated by mean of comparison with analytical and experimental results [10].

The load case considered for this analysis is N1.0 defined in GL, corresponding to a regular power production, the verifications of fatigue life having been made with this case. The study carried out is a static analysis of first order (without considering large displacements).

The longitudinal normal efforts per unit length (the resultant of the longitudinal normal stresses through the

thickness of the laminate) will be taken as a reference to compare the different configurations considered, which from now on will be denoted by  $N_x$  (Fig. 13).

The values of  $N_x$  obtained for the load case N1.0 and for the original geometry of the blade are represented in Fig. 14, for the face in tension of the blade, where the damages were observed. The zone represented is the one where  $N_x$  reaches the highest values, due to the presence of the concentrator. It has to be clarified that, quantitatively speaking, the values of  $N_x$  calculated have meaning only for comparison purposes between similar meshes, since the theoretical nominal value of  $N_x$  at the vertex of the re-entrant corner is infinite, the values obtained being strongly dependent on the discretization carried out at the neighbourhood of the corner.

It can also be observed that the trailing edge zone, within the aerodynamic part of the blade, does not transmit significant loads in the longitudinal direction, in comparison with the zone of the leading edge. For this reason there are almost no unidirectional laminas oriented longitudinally in the trailing edge. This is an important fact to be taken into account when modifying the local geometry of the corner.

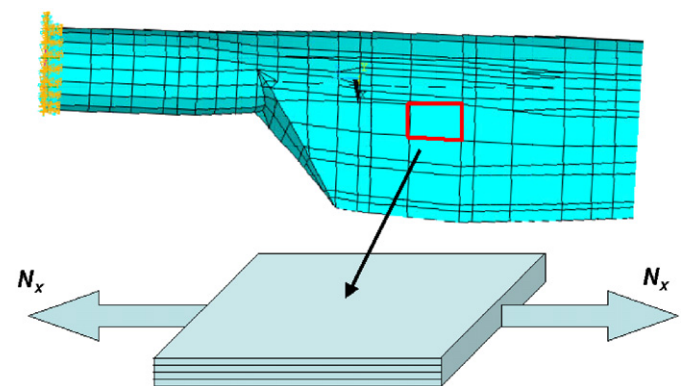


Fig. 13. Scheme of the longitudinal normal efforts.

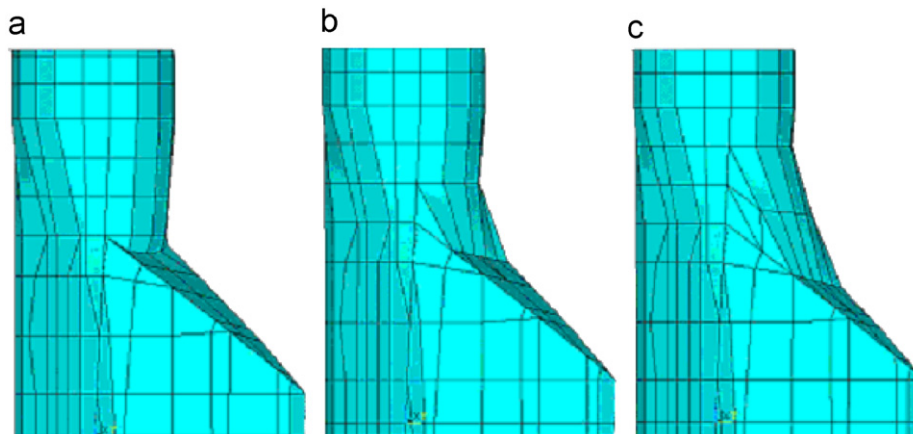


Fig. 12. (a) Original geometry, (b) modified geometry 1 and (c) modified geometry 2.

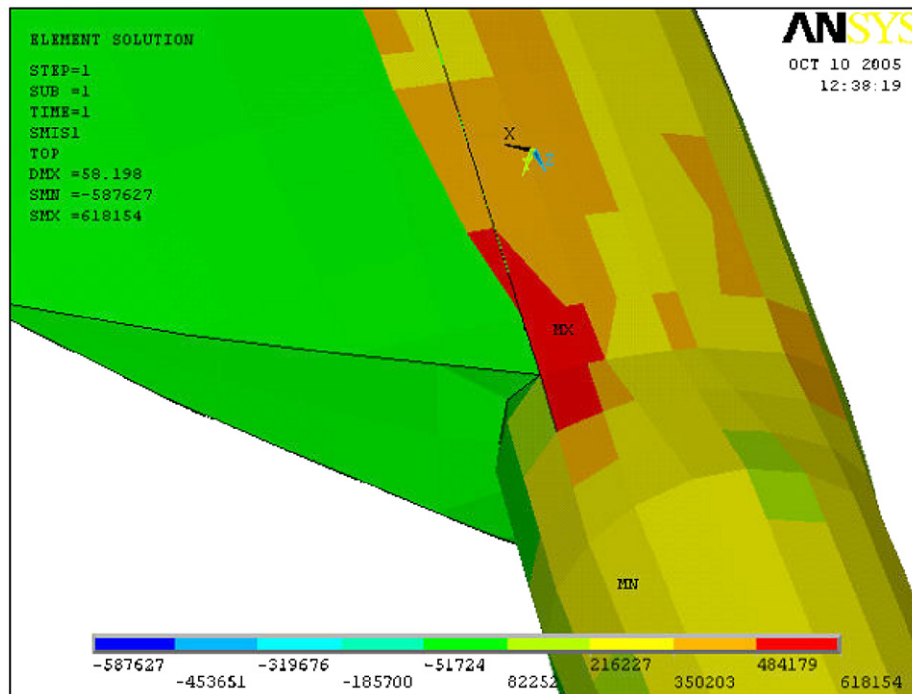


Fig. 14.  $N_x$  efforts in the original configuration of the blade.

## 5.2. Analysis of modifications

In order to release the stress state in the zone of influence of the concentrator, a lateral triangle of resistant material that smoothes the re-entrant corner (see Fig. 12b) in the zone where the crack appeared will be introduced. This modification obviously goes along with the modification of the elements that connect the root with the cover. In detail, the modification of the original model consists of:

1. The creation of the elements that define the lateral triangles.
2. The redefinition of the stacking sequence of the elements of the cover that contact with the root.
3. The modification of the laminates in the elements adjacent to the triangular lateral element in the longitudinal direction.

In order to have a triangle with suitable mechanical behaviour, a similar laminate to that existing in the nearest elements at the root has been considered. The structure of the laminate of the triangle is described in Table 4.

In the damaged area where in the repaired blade two identical laminates will appear superimposed (one corresponding to the original laminate and the other corresponding to the added triangle), only the properties corresponding to the laminate of the added triangle have been considered in the model. This is a conservative hypothesis which does not consider the residual properties of the original laminate which will be affected by some fibre breaking and general damage.

Table 4  
Triangle laminate

Lamina	Weight by unit area (g/m <sup>2</sup> )
1 MAT	200
3 NUFF (0°)	1450
1 BIAx (±45°)	300
3 NUFF (0°)	1450
1 BIAx (±45°)	300
6 NUFF (0°)	1450
1 MAT	400

The complete laminate of the triangle has been added in the model to the laminate of the adjacent elements of the non-damaged area (which originally did not contain NUFF), to give continuity to the resistance of the triangle, thus creating an alternative path for the transmission of longitudinal stresses, which find a path of connection with the contiguous laminates that have a significant resistance capacity.

The geometry of the cover is modified to adapt it to the geometry of the lateral triangles. In addition, the laminate of the cover is modified to make it more resistant and to prevent the appearance of the crack observed in the inspected blades. The laminate defined on the elements of the cover is defined in Table 5.

The values of  $N_x$  obtained for load case N1.0 and for the modified geometry (configuration 1) are shown in Fig. 15. The modification produces two effects on the stress state. First a reduction in the level of stress at the neighbourhood of the corner of the original configuration, and second the



redistribution of the stresses introduced throughout the triangle and the adjacent elements in longitudinal direction. These effects will be evaluated quantitatively in Section 5.3.

A second modification is considered (configuration 2), the only difference between the two modifications being the dimension of the triangle introduced, which is greater in this modified configuration 2. The stacking sequence of the laminate of the elements that define the triangle responds to that indicated in Table 4, whereas the laminate defined on the elements of the cover is that shown in Table 5. The modification of the laminates of the adjacent elements now affects a greater number of elements than in the type 1 modification.

The values of  $N_x$  obtained for the load case N1.0 and for the modified geometry (configuration 2) are represented in Fig. 16. Observation of Fig. 16 leads to the same conclusions as in the case of Fig. 16, the redistribution of stresses in the elements adjacent to the triangle introduced being even greater than in configuration 1.

Table 5  
Laminate of the cover

Lamina	Weight by unit area (g/m <sup>2</sup> )
1 MAT	200
3 NUFF (0°)	1450
1 BIAx (±45°)	300
2 NUFF (0°)	1450
1 MAT	200

### 5.3. Evaluation of results

To evaluate the influence of the modifications performed in the stress state, it has to be taken into account that the comparison of the results has to be made far enough from the vertex of the corner to leave the results unaffected by the nominal corner singularity. Additionally, the value of  $N_x$  must be compared in the area where the damage appeared, this area being represented in Fig. 17, over the original configuration geometry.

In Figs. 18–20 the evolution of the longitudinal average stress  $\sigma_x$  ( $\sigma_x = N_x/t$ ,  $N_x$  taken from the centroid of the element and  $t$  being the thickness of the laminate) as a function of the distance to the corner is shown for the different configurations. The evolutions corresponding to the elements placed at both sides (root and blade) of the line of study have been represented, though the observed failure is located on the side of the aerodynamic zone (blade).

From Figs. 18–20 the following observations are deduced:

1. Although the qualitative evolution of the stresses in the elements at both sides of the line under study (root and blade) is similar, the difference in thickness between the laminates of these elements (corroborated during the inspection of the blades, see Section 2) generates a higher stress level in the elements of the side of the aerodynamic zone of the blade than in the elements of the side next to the root. The thicknesses along the lines under study (root and blade) are listed in Table 6.

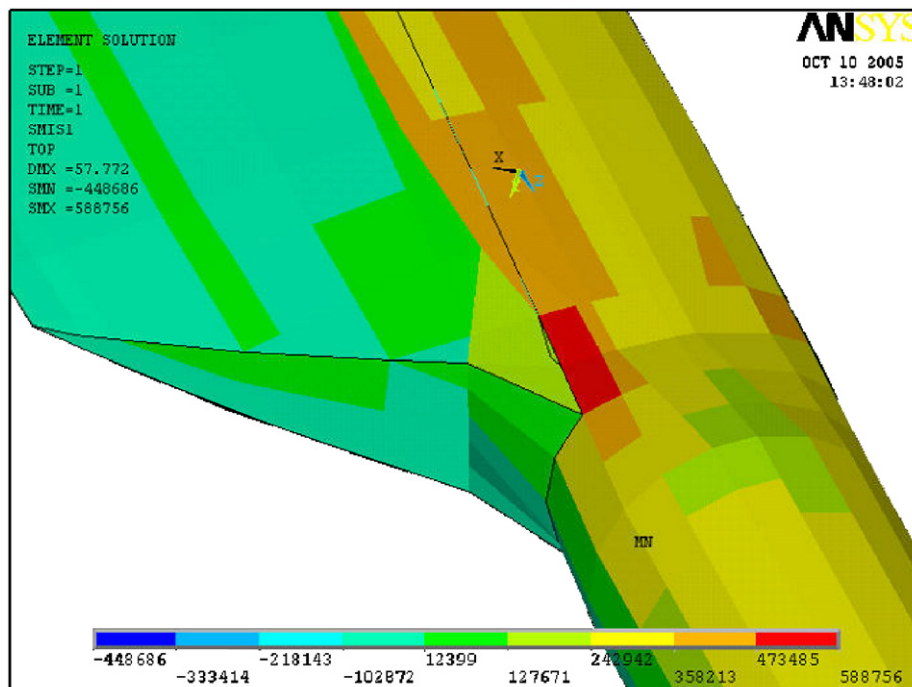


Fig. 15.  $N_x$  efforts corresponding to configuration 1.



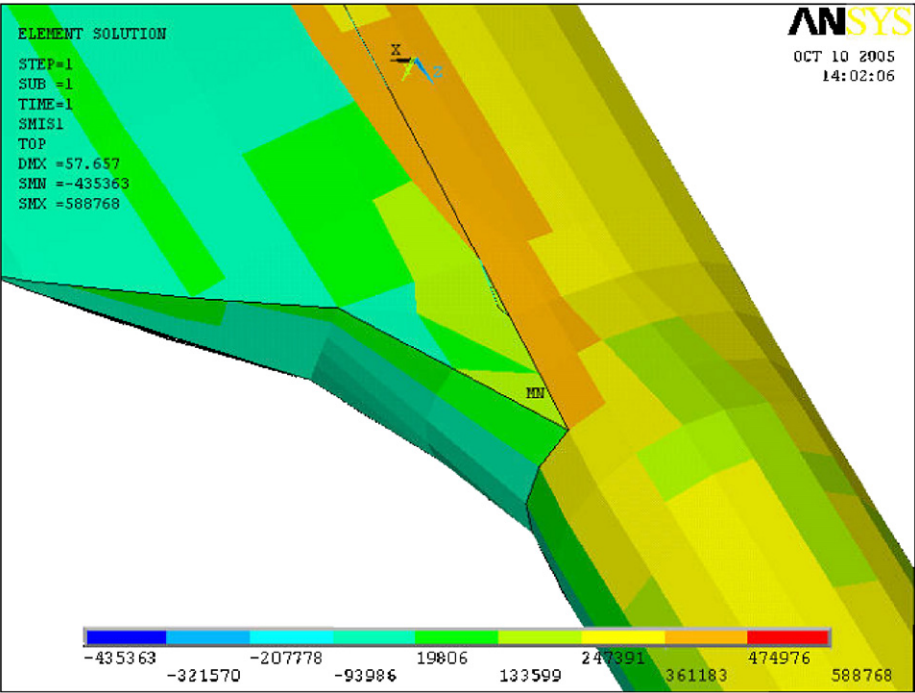


Fig. 16.  $N_x$  efforts corresponding to configuration 2.

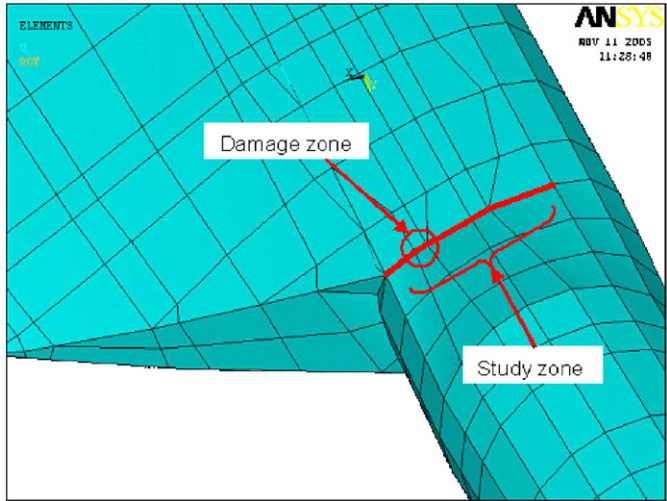


Fig. 17. Line under study and damage zone locations.

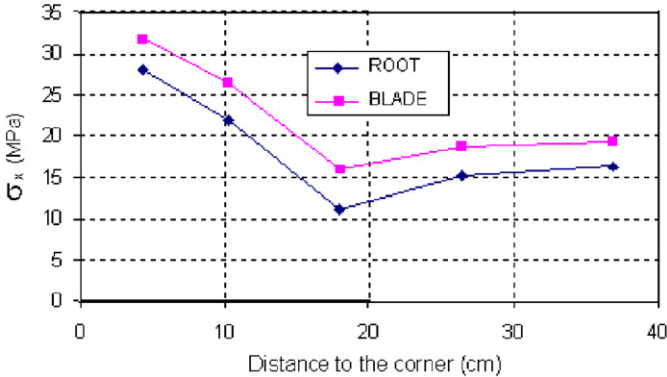


Fig. 18. Evolution of the stress  $\sigma_x$  in the original configuration.

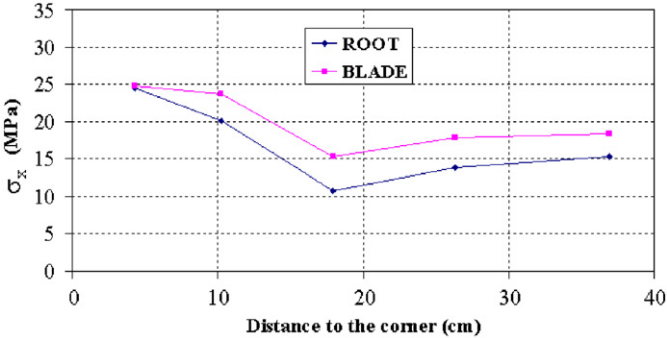


Fig. 19. Evolution of the stress  $\sigma_x$  in configuration 1.

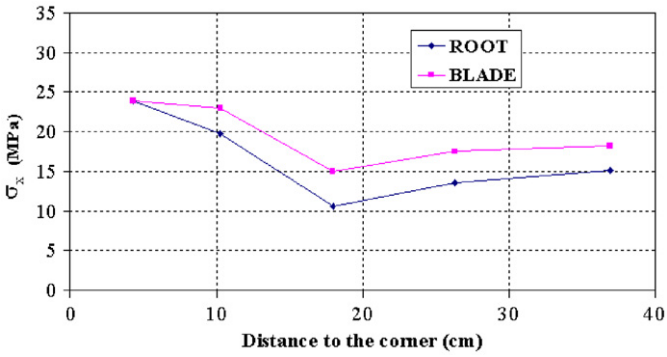


Fig. 20. Evolution of the stress  $\sigma_x$  in configuration 2.

2. The evolution of the stress in the original configuration quantitatively demonstrates the presence of a stress concentrator. The introduction of the triangles in the modified configurations attenuates this concentration,

reducing as well as the value of the stress at the damaged zone.

3. Far away from the concentrator, the distribution of stress is not affected significantly in the modified configurations.
4. The stress level found in the zone far from the concentrator (see Figs. 18–20) adjusts reasonably well to the value of the previously obtained nominal stress in this zone using the Strength of Materials approach.

### 5.3.1. Fatigue life estimation for the modified configurations

With a view to evaluating the influence of the obtained stress variations on the fatigue life of the modified configurations of the blade with respect to the original one, the calculation procedure by means of the simplified load spectrum set out in Section 4.1 will be used. To do this, the nominal stress that originates the failure by fatigue in a period of five years (corresponding to the original configuration) will be considered. This value will be affected by the stress decrements associated to each modified configuration.

The results of the analysis appear in Table 7, where the stress decrements between the modified configurations and the original one, as well as the increases in life with respect to the life of 5 years taken as a reference for the original

configuration, are shown. The results show the improvement in fatigue life obtained with the modifications carried out: the greater the size of the triangle, the greater the increase in life, as expected.

### 5.3.2. Parametric study

To investigate the influence of the configuration of the laminates used on the increase of fatigue life, variations on the two modified configurations that consist of increasing or decreasing, respectively, the number of unidirectional layers present in the laminates involved in the modification have been studied. The reference laminate configurations are those previously described in Tables 4 and 5. In particular, variations of  $\pm 2$  and  $\pm 4$  unidirectional layers (NUFF 1450 g/m<sup>2</sup>) have been considered, the results being shown in Table 8.

From the results of Table 8 it can be observed that:

1. The increase in the number of NUFF layers causes an increase in life, the variation being slightly more pronounced when NUFF layers are eliminated from the reference laminate in comparison with the case where layers are added.
2. As was previously seen, the greatest increase in life was obtained with the greatest size of the triangle. In addition, the greater influence of this effect on fatigue life in comparison with the variation in the laminate studied can now be observed.

Table 6  
Thicknesses of the laminates

Distance to the corner (cm)	Root thickness (cm)	Blade thickness (cm)
4.31	1.99	1.94
10.26	2.18	1.94
17.97	2.37	1.89
26.34	2.13	1.89
36.91	1.99	1.76

Table 7  
Stress variations and fatigue lives for the two modifications of the blade

Configuration	$\Delta$ Stress (MPa) (%)	$\Delta$ Life (years)
Modification 1	−2.73 (10.33%)	4.8
Modification 2	−3.37 (12.75%)	6.6

Table 8  
Stress and fatigue life variation for the laminate modifications

Configuration	Reference				
	Laminate −4	Laminate −2	Laminate	Laminate +2	Laminate +4
Modification 1					
$\Delta\sigma$ (MPa)	−2.46	−2.61	−2.73	−2.82	−2.89
$\Delta$ Life (years)	4.2	4.6	4.8	5.1	5.3
Modification 2					
$\Delta\sigma$ (MPa)	−3.03	−3.22	−3.37	−3.48	−3.58
$\Delta$ Life (years)	5.6	6.1	6.6	6.9	7.2

## 6. Materialization of the modifications in the concentrator geometry

Due to the fact that the suggested modifications entail the addition of a triangular surface in the concentrator zone, it is necessary to guarantee the structural continuity of this piece with the rest of the blade. This continuity can be guaranteed by using greater dimensions to those of the triangle itself, in order to allow, by means of an overlapping, the bonding over the surface of the blade (see Fig. 21).

Since the laminate of the triangle contains a considerable number of layers, the appropriate way to build up the laminate requires each lamina to have direct bonding with the surface of the blade, which means that each lamina

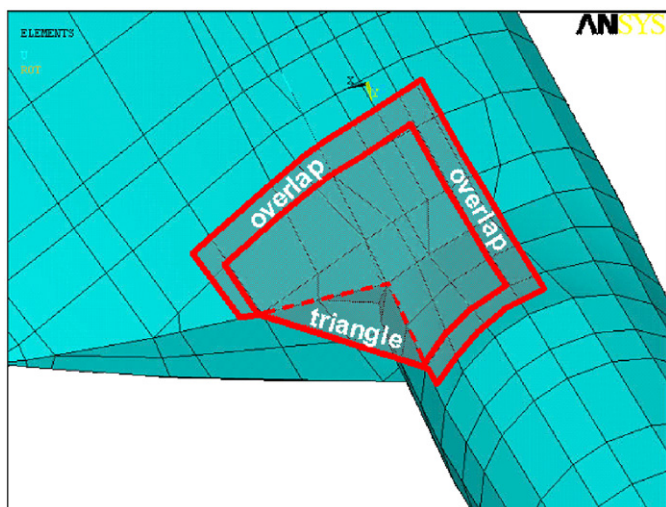


Fig. 21. Scheme of the configuration of reinforcement and the overlaps.

must overlap the previous one by a certain length along the whole periphery (see Fig. 21). In this way a progressive transmission of loads takes place from the blade to the triangular surface so that the surface can develop its resistant function.

In relation to the geometry of the reinforcement layers, a geometry in trapezoidal form, as an extension of the triangle, has been chosen.

The overlap lengths chosen for the longitudinal direction (minimum 5 cm) guarantee the correct load transmission to reinforcement layers, so that each lamina can completely develop its resistance capacity in tension by means of the fibres, without being limited by the shear strength of the bonding area with the blade. In transverse direction, where the efforts are much smaller, the overlap lengths (minimum 2 cm) are chosen to generate a smooth transition of the laminates.

## 7. Conclusions

The inspection of the blade revealed the following damages:

- Damage appearing in the form of a crack that affected the (non-resistant) superficial laminate, extending over the influence zone of the concentrator and with its likely origin at the corner between the cover and the root.
- Damage in the form of a crack that affected the resistant laminate, extending over the zone where there was an abrupt change in the thickness of the laminate.
- Lack of bonding, lack of resin and diverse manufacture defects.

The nature of the observed failure seems to be due to a fatigue mechanism. The configuration of the observed cracks seems to indicate that first a superficial crack (Fig. 10a) appeared, probably around the weakest point (corner between the cover and the root) due to the stress

concentration, this crack progressing throughout the superficial layer and inducing delamination between this superficial layer and the resistant laminate. Later on, in the zone where there was an abrupt change of thickness, the presence of the superficial crack together with the effect of the concentrator and the effect of the change in thickness gave rise to the stress state necessary to generate a crack in the resistant laminate (Fig. 10b), which completely broke the laminate, as is observed in Fig. 10c.

By means of the simplified procedure of the standard GL, a calculation of fatigue life for the laminate corresponding to the zone of failure has been carried out. It has been deduced that it is plausible that this laminate reached a fatigue life in the order of 5 years, considering that it was subjected to the combined effect of the presence of the superficial crack, the effect of the geometric concentrator and the effect of the change in thickness, all this giving rise to an amplification of the nominal stress at the zone considered. Additionally, the presence of diverse defects of manufacture could, in any case, contribute to a decrement in the fatigue life of the element.

To design a suitable repair, the influence that the geometry of the concentrator that appears in the transition from the root to the aerodynamic zone has on the stress state, and consequently on the fatigue life of the blade, has been studied. It has been found that the inclusion of a triangular surface “filling up” the corner that generates the stress concentration, significantly releases the stress state in the zone where the failure has been observed and provides an improvement in the fatigue life of the blade.

The influence of the size of the triangle has been analysed as well as the influence of the amount of unidirectional layers in the laminate of these triangles. It has been observed that the size of the triangle is the dominant parameter in the behaviour of this type of reinforcement, the greatest increases in fatigue life corresponding to the triangle of greatest size. The variations in life associated to the number of unidirectional layers are of an inferior level.

## References

- [1] Sutherland HJ. On the fatigue analysis of wind turbines. SAND99-0089, Sandia National Laboratories, Albuquerque, NM; 1999. <<http://www.prod.sandia.gov/cgi-bin/techlib/access-control.pl/1999/990089.pdf>>.
- [2] Sutherland HJ, Mandell JF. Effect of mean stress on the damage of wind turbine blades. In: 2004 ASME wind energy symposium, AIAA/ASME; 2004. p. 32–44.
- [3] Mandell JF, Samborsky DD. DOE/MSU composite material fatigue database: test methods, materials and analysis. SAND97-3002, Sandia National Laboratories, Albuquerque, NM; 1997. <<http://www.prod.sandia.gov/cgi-bin/techlib/access-control.pl/1997/973002.pdf>>.
- [4] Andersen SI, Bach PW, Bonnee WJA, Kensche CW, Lilholt H, Lystrup A, et al. Fatigue of materials and components for wind turbine rotor blades. European Commission, Directorate-General XII, science, research and development, EUR 16684 EN, Brussels; 1996.
- [5] Germanischer Lloyd, rules and regulations IV—non marine technology, part I—wind energy. Hamburg: Germanischer Lloyd; 1999.

- [6] Kong C, Bang J, Sugiyama Y. Structural investigation of composite wind turbine blade considering various load cases and fatigue life. *Energy* 2005;30:2101–14.
- [7] Kensché CW. Fatigue of composites for wind turbines. *Int J Fatigue* 2006;28:1363–74.
- [8] Kong C, Kim T, Han D, Sugiyama Y. Investigation of fatigue life for a medium scale composite wind turbine blade. *Int J Fatigue* 2006;28:1382–8.
- [9] Shokrieh MM, Rafiee R. Simulation of fatigue failure in a full composite wind turbine blade. *Compos Struct* 2006;74(3):332–42.
- [10] Cañas J, Marín JC, Barroso A, París F. On the use of strength of materials models and finite element models in wind turbine blades design (Sobre el uso de modelos de resistencia de materiales y modelos de elementos finitos en el diseño de palas de aerogenerador). In: *Proceedings of the MATCOMP-99*, Benalmádena, Spain; 1999. p. 271–8 [in Spanish].
- [11] Tsai SW. *Composites design*. Dayton, OH: Think Composites; 1988.
- [12] Tan SC. A progressive failure model for composite laminates containing openings. *J Compos Mater* 1991;25:556–77.
- [13] Paluch B. A software for design and calculation of wind turbine composite rotor blades. In: *European community wind energy conference*, 8–12 March 1993. p. 559–62.
- [14] Pilkey WD. *Formulas for stress, strain, and structural matrices*. New York: Wiley; 1994. p. 286–7.
- [15] ANSYS, Swanson Analysis System, Inc.; 2003.